

Temperature and finite-size effects in collective modes of superfluid Fermi gases

M. Grasso,^{1,2} E. Khan,² and M. Urban²

¹*Dipartimento di Fisica ed Astronomia and INFN, Via Santa Sofia 64, I-95123 Catania, Italy*

²*Institut de Physique Nucléaire, Université Paris-Sud, IN2P3-CNRS, 91406 Orsay Cedex, France*

We study the effects of superfluidity on the monopole and quadrupole collective excitations of a dilute ultra-cold Fermi gas with an attractive interatomic interaction. The system is treated fully microscopically within the Bogoliubov-de Gennes and quasiparticle random-phase approximation methods. The dependence on the temperature and on the trap frequency is analyzed and systematic comparisons with the corresponding hydrodynamic predictions are presented in order to study the limits of validity of the semiclassical approach.

PACS numbers: 03.75.Ss, 21.60.Jz

I. INTRODUCTION

Dilute gases of alkaline fermionic and bosonic atoms are superfluid at very low temperature: Bose-Einstein condensates have been obtained in the case of bosonic atoms [1], while condensation of molecules (made out of two atoms) has been observed in the case of fermionic atoms [2]. For fermionic atoms in the weakly interacting regime ($k_F|a| \ll 1$, where k_F is the Fermi momentum and a the s-wave scattering length) BCS superfluidity is expected in the case of attractive interatomic interaction ($a < 0$).

A striking experimental evidence for BCS superfluidity is still missing, even though various signals which would be coherent with a superfluid behavior have been observed in some experiments: the anisotropic expansion of the gas after releasing it from the trap [3], the measurement of the gap [4], the measurement of the frequencies and damping rates of the breathing modes [5].

However, the gap has been actually measured only in the strongly interacting regime and no experimental values exist for the weakly interacting case. The anisotropic expansion on the one hand and the frequencies of the breathing modes on the other hand can be predicted within a hydrodynamic approach for a superfluid gas [6, 7, 8]. In both cases the experimental observations agree very well with the hydrodynamic predictions, and this could actually be considered as an evidence for superfluidity. However, the predictions for a superfluid gas are the same as those for a normal gas in the presence of collisions. It is true that at the very low temperatures achieved in these experiments Pauli principle is expected to inhibit collisions. However, the experimental measurements have been performed during the expansion of the gas after releasing it from the trap. In such a situation momentum space deformations are possible and collisions can survive even at very low temperatures. So far, it has not been possible to completely control this problem from an experimental point of view and, for this reason, no firm conclusions about superfluidity can actually be drawn.

Another limitation is related to the hydrodynamic approach: hydrodynamics can be safely applied only

within the limits of validity of semiclassical approaches, $\Delta \gg \hbar\Omega$, where Δ is the pairing gap and Ω is the trapping frequency. Effects from the finite size and inhomogeneity, governed by the finite trap frequency Ω , are neglected. Moreover, the hydrodynamic formalism has been developed so far only for the case of zero temperature ($T = 0$).

In this article we deal with the excitation spectra in the normal and superfluid phases of a dilute Fermi gas and we analyze how these spectra are affected by superfluidity, both in hydrodynamic and microscopic descriptions. In order to study excitations similar to those observed experimentally (the breathing modes) we focused our attention on the monopole and quadrupole modes. However, while the breathing modes have been observed for a cigar-shaped gas (and the radial and axial frequencies have been measured), we restrict our analysis to a spherical gas for the sake of numerical tractability. Moreover, while the experiment of Ref. [5] has been done for a strongly interacting gas, we treat a weakly interacting system.

We analyze the excitation spectra within a finite-temperature mean-field approach which provides a microscopic treatment for the system. The Bogoliubov-de Gennes (BdG) equations [9] are solved for the ground state and the excitations are treated within the quasiparticle random-phase approximation (QRPA) [10]. This approach has already been developed for atomic Fermi gases in Ref. [11], where the spin-dipole and the quadrupole modes have been analyzed. On the other hand, the monopole modes have already been studied and compared to a schematic model in Ref. [12].

In the present work we want to study systematically the effects related to the temperature and to the trap frequency of the system. In particular, we compare our results with the corresponding hydrodynamic ones in order to check the validity of the semiclassical approach. In addition to the strength distributions related to the excitation spectra, we also present the transition densities which can give important information on nature of the collective modes.

The article is organized as follows. In Sect. II we briefly sketch the quantum mechanical and semiclassical formalisms to describe collective modes in the superfluid

phase and in the normal phase in the collisionless limit. In Sect. III results for the monopole and quadrupole excitations are shown: the dependence on the temperature and on the frequency of the trap are studied. In Sect. IV we draw our conclusions.

II. QUANTUM MECHANICAL AND SEMICLASSICAL FORMALISM

In this section we will briefly review the theoretical description of collective modes in trapped Fermi gases. As already mentioned in the introduction, one has to distinguish between quantum mechanical (“microscopic”) and semiclassical approaches. The fully quantum mechanical calculation consists in solving the QRPA equations, which are the small-amplitude limit of the time-dependent BdG equations. At present such calculations are available only for systems containing up to $\sim 10^4$ atoms in the case of a spherically symmetric trap. These conditions are quite far from the experimental ones, corresponding to particle numbers of $\sim 10^5 - 10^6$ particles in a cigar-shaped trap. Up to now, the “realistic” conditions can only be treated within semiclassical approaches. The simplest semiclassical approach is the hydrodynamic theory. This theory is valid in the superfluid phase at zero temperature, since the pairing correlations keep the Fermi surface spherical during the collective motion of the system. However, hydrodynamics fails at non-zero temperature, unless the local equilibrium can be ensured by collisions. Since we are interested in the weakly interacting regime, the collision rate $1/\tau$ is very small compared to the frequency of the trap. In this “collisionless” regime, the Fermi surface becomes locally deformed during the collective oscillation. This cannot be described by hydrodynamics, but requires a description in the framework of the Vlasov equation. The latter is valid in the normal phase, i.e., above the critical temperature T_c . In the intermediate temperature range $0 < T < T_c$, a semiclassical theory is still missing.

A. Quantum mechanical formalism (QRPA)

The QRPA method has already been applied to trapped Fermi gases in the weakly [11] as well as in the strongly interacting regime [13] and here we will only give a short summary.

We consider a gas of atoms with mass m in a spherical harmonic trap with frequency Ω , assuming that the atoms equally occupy two hyperfine states $\sigma = \uparrow, \downarrow$. Because of the low temperature and density of the gas, the interaction between the atoms can be chosen as a zero-range interaction and parametrized by the s-wave atom-atom scattering length a . In order to simplify the notation, we will express all quantities in harmonic oscillator (HO) units, i.e., frequencies in units of Ω , energies in units of $\hbar\Omega$, temperatures in units of $\hbar\Omega/k_B$, and lengths

in units of the oscillator length $l_{HO} = \sqrt{\hbar/(m\Omega)}$. Furthermore, instead of the scattering length we will use the coupling constant $g = 4\pi a/l_{HO}$ as parameter of the interaction strength.

As mentioned above, the QRPA describes small-amplitude oscillations around the equilibrium state within the BdG formalism. Therefore, the first step consists in solving the BdG equations [9]

$$\begin{aligned} [H_0 + W(r)]u_{nlm}(\mathbf{r}) + \Delta(r)v_{nlm}(\mathbf{r}) &= E_{nl}u_{nlm}(\mathbf{r}), \\ \Delta(r)u_{nlm}(\mathbf{r}) - [H_0 + W(r)]v_{nlm}(\mathbf{r}) &= E_{nl}v_{nlm}(\mathbf{r}) \end{aligned} \quad (1)$$

for the static case. In this way we obtain a set of quasiparticle energies E_{nl} and wave-functions u_{nlm} and v_{nlm} . In Eq. (1), H_0 denotes the hamiltonian of the non-interacting HO minus the chemical potential μ ,

$$H_0 = \frac{1}{2}(-\nabla^2 + r^2) - \mu, \quad (2)$$

while the interaction is accounted for in a self-consistent way through the Hartree potential W and the pairing field Δ . Due to spherical symmetry, the wave functions can be written as

$$u_{nlm}(\mathbf{r}) = u_{nl}(r)Y_{lm}(\theta, \phi), \quad (3)$$

$$v_{nlm}(\mathbf{r}) = v_{nl}(r)Y_{lm}(\theta, \phi). \quad (4)$$

The quantum numbers l and m are the angular momentum and its projection, while n numbers different states having the same l and m . In practice, the diagonalization of Eq. (1) is done in a truncated harmonic oscillator basis, containing the eigenfunctions of the trapping potential up to a certain HO energy $E_C = N_C + \frac{3}{2}$, i.e.,

$$2(n-1) + l \leq N_C. \quad (5)$$

The self-consistency relates W and Δ to the wave functions u and v . The mean field W is just proportional to the density, i.e.,

$$W(\mathbf{r}) = g \sum_{nl}^{N_C} \frac{2l+1}{4\pi} \{v_{nl}^2(r)[1 - f(E_{nl})] + u_{nl}(r)f(E_{nl})\}, \quad (6)$$

where

$$f(E) = \frac{1}{e^{E/T} + 1} \quad (7)$$

denotes the Fermi function. The Hartree field is independent of the cutoff N_C if the latter is taken sufficiently large. The calculation of the pairing field Δ , however, is more complicated. The zero-range interaction leads to a divergence which in the case of uniform systems can be regularized in a standard way by renormalizing the scattering length. This regularization method has been generalized to the case of trapped systems by Bruun et al. [14] and developed further by Bulgac and Yu [15] and

two of the authors [16]. As a result, the pairing field can be written as

$$\Delta(\mathbf{r}) = -g_{\text{eff}}(r) \sum_{nl} \frac{2l+1}{4\pi} u_{nl}(r) v_{nl}(r) [1 - 2f(E_{nl})], \quad (8)$$

with an effective coupling constant g_{eff} which allows to include the contribution from states beyond the cutoff N_C within the Thomas-Fermi approximation (TFA). The explicit expression for g_{eff} reads

$$\frac{1}{g_{\text{eff}}(r)} = \frac{1}{g} + \frac{1}{2\pi^2} \left(\frac{k_F(r)}{2} \ln \frac{k_C(r) + k_F(r)}{k_C(r) - k_F(r)} - k_C(r) \right), \quad (9)$$

where k_F and k_C denote the local Fermi and cutoff momenta, respectively:

$$k_F(r) = \sqrt{2\mu - r^2 - 2W(r)}, \quad (10)$$

$$k_C(r) = \sqrt{2N_C + 3 - r^2}. \quad (11)$$

Once the static BdG equations are solved, we can calculate the linear response of the system to a small time-dependent perturbation. Following Ref. [11], we have to compute the QRPA response function Π , which is a 4×4 matrix built out of 16 correlation functions:

$$\Pi(\omega, \mathbf{r}, \mathbf{r}') = \begin{pmatrix} \langle\langle \hat{\rho}_\uparrow \hat{\rho}_\uparrow \rangle\rangle & \langle\langle \hat{\rho}_\uparrow \hat{\rho}_\downarrow \rangle\rangle & \langle\langle \hat{\rho}_\uparrow \hat{\chi} \rangle\rangle & \langle\langle \hat{\rho}_\uparrow \hat{\chi}^\dagger \rangle\rangle \\ \langle\langle \hat{\rho}_\downarrow \hat{\rho}_\uparrow \rangle\rangle & \langle\langle \hat{\rho}_\downarrow \hat{\rho}_\downarrow \rangle\rangle & \langle\langle \hat{\rho}_\downarrow \hat{\chi} \rangle\rangle & \langle\langle \hat{\rho}_\downarrow \hat{\chi}^\dagger \rangle\rangle \\ \langle\langle \hat{\chi} \hat{\rho}_\uparrow \rangle\rangle & \langle\langle \hat{\chi} \hat{\rho}_\downarrow \rangle\rangle & \langle\langle \hat{\chi} \hat{\chi} \rangle\rangle & \langle\langle \hat{\chi} \hat{\chi}^\dagger \rangle\rangle \\ \langle\langle \hat{\chi}^\dagger \hat{\rho}_\uparrow \rangle\rangle & \langle\langle \hat{\chi}^\dagger \hat{\rho}_\downarrow \rangle\rangle & \langle\langle \hat{\chi}^\dagger \hat{\chi} \rangle\rangle & \langle\langle \hat{\chi}^\dagger \hat{\chi}^\dagger \rangle\rangle \end{pmatrix}, \quad (12)$$

with the short-hand notation

$$\langle\langle \hat{A} \hat{B} \rangle\rangle = -i \int_0^\infty \frac{dt}{2\pi} e^{i\omega t} \langle [\hat{A}(t, \mathbf{r}), \hat{B}(0, \mathbf{r}')] \rangle, \quad (13)$$

where $\langle \rangle$ means the thermal average. The operators of the normal and anomalous densities, $\hat{\rho}$ and $\hat{\chi}$, are defined in terms of the field operators $\hat{\psi}$ and $\hat{\psi}^\dagger$ as follows:

$$\hat{\rho}_\sigma(t, \mathbf{r}) = \hat{\psi}_\sigma^\dagger(t, \mathbf{r}) \hat{\psi}_\sigma(t, \mathbf{r}), \quad (14)$$

$$\hat{\chi}(t, \mathbf{r}) = \hat{\psi}_\downarrow(t, \mathbf{r}) \hat{\psi}_\uparrow(t, \mathbf{r}). \quad (15)$$

In order to obtain Π , we first compute the free or unperturbed response function Π_0 , which is defined analogously to Eq. (12), but which does not include the effect of interactions between the quasiparticles. Thus Π_0 can be obtained by replacing the field operators $\hat{\psi}$ in Eqs. (14) and (15) by

$$\hat{\psi}_\sigma(t, \mathbf{r}) = \sum_{nlm} [b_{nlm\sigma} u_{nlm}(\mathbf{r}) e^{iE_{nl}t} - \sigma b_{nlm-\sigma}^* v_{nlm}^*(\mathbf{r}) e^{-iE_{nl}t}], \quad (16)$$

where \hat{b} and \hat{b}^\dagger are annihilation and creation operators of non-interacting quasiparticles. Inserting the resulting expressions into Eq. (12) and using the relations

$\{b_\alpha, b_\beta\} = \{b_\alpha^\dagger, b_\beta^\dagger\} = 0$, $\{b_\alpha, b_\beta^\dagger\} = \delta_{\alpha\beta}(1 - f(E_\alpha))$, and $\langle b_\alpha^\dagger b_\beta \rangle = f(E_\alpha) \delta_{\alpha\beta}$, we obtain explicit expressions for the 16 functions contained in Π_0 in terms of the u and v functions and the quasiparticle energies obtained from Eq. (1).

Due to the spherical symmetry of the trap and the rotational invariance of the interaction, excitations with different angular momenta do not mix. Therefore it is useful to decompose Π_0 into contributions of different angular momenta:

$$\Pi_0(\omega, \mathbf{r}, \mathbf{r}') = \sum_{LM} \Pi_{0L}(\omega, r, r') Y_{LM}(\theta, \phi) Y_{LM}^*(\theta', \phi'). \quad (17)$$

The QRPA response Π_L for angular momentum L can now be obtained from the quasiparticle response Π_{0L} by solving the Bethe-Salpeter integral equation

$$\Pi_L(\omega, r, r') = \Pi_{0L}(\omega, r, r') + \int_0^\infty dr'' r''^2 \Pi_{0L}(\omega, r, r'') G \Pi_L(\omega, r'', r'), \quad (18)$$

where G accounts for the residual interaction between the quasiparticles:

$$G = \begin{pmatrix} 0 & g & 0 & 0 \\ g & 0 & 0 & 0 \\ 0 & 0 & 0 & g \\ 0 & 0 & g & 0 \end{pmatrix}. \quad (19)$$

When calculating the 16 functions contained in Π_{0L} , one observes that two of them, namely those related to $\langle\langle \hat{\chi}^\dagger \hat{\chi} \rangle\rangle$ and $\langle\langle \hat{\chi} \hat{\chi}^\dagger \rangle\rangle$, are divergent for $N_C \rightarrow \infty$. This divergence has the same origin as that of the pairing field. Bruun and Mottelson [11] therefore suggested to use the same pseudopotential method as for the regularization of the pairing field in order to remove the divergence. However, it is not clear how in their prescription, Eq. (7) in Ref. [11], the contribution of states beyond the cutoff N_C can be approximated (as we did in the case of the pairing field by using the TFA), which is crucial for having convergence at reasonable values of the cutoff N_C . We therefore propose a simplified prescription: when calculating Π_{0L} , we have to restrict the sum to states below the cutoff, $2(n-1) + l \leq N_C$. To compensate the resulting cutoff dependence, the interaction in the pairing channel must be replaced by the effective coupling constant given in Eq. (9). Thus, we replace G in Eq. (18) by $G_{\text{eff}}(r'')$, which is defined by

$$G_{\text{eff}}(r) = \begin{pmatrix} 0 & g & 0 & 0 \\ g & 0 & 0 & 0 \\ 0 & 0 & 0 & g_{\text{eff}}(r) \\ 0 & 0 & g_{\text{eff}}(r) & 0 \end{pmatrix}. \quad (20)$$

One can show that, in the case of a uniform system, this simplified prescription coincides with the pseudopotential method in the limit of excitations with long wavelengths

and low frequencies. We have checked the convergence of the results using this regularization prescription.

Finally, we have to say how physical quantities of interest can be extracted from the correlation function Π . To that end it is useful to look at the spectral representation

$$\sum_{\sigma\sigma'} \langle \langle \hat{\rho}_\sigma \hat{\rho}_{\sigma'} \rangle \rangle = \int d\omega' \frac{S(\omega', \mathbf{r}, \mathbf{r}')}{\omega - \omega' + i\varepsilon}, \quad (21)$$

with

$$\begin{aligned} S(\omega, \mathbf{r}, \mathbf{r}') &= -\frac{1}{\pi} \sum_{\sigma\sigma'} \text{Im} \langle \langle \hat{\rho}_\sigma \hat{\rho}_{\sigma'} \rangle \rangle \\ &= (1 - e^{-\omega/T}) \sum_{ij} \frac{e^{-E_i/T}}{Z} \delta(\omega - E_j + E_i) \\ &\quad \times \sum_{\sigma\sigma'} \langle i | \hat{\rho}_\sigma(\mathbf{r}) | j \rangle \langle j | \hat{\rho}_{\sigma'}(\mathbf{r}') | i \rangle, \end{aligned} \quad (22)$$

where $|i\rangle$ and $|j\rangle$ are eigenstates of the many-body hamiltonian with total energies E_i and E_j , respectively, and $Z = \sum_i \exp(E_i/T)$. In the present QRPA formalism Eq. (22) is evaluated using the four upper left elements of the Π response function (12), obtained with Eq. (18).

In this paper we will consider excitation operators of the form

$$V_1(t, \mathbf{r}) \propto r^2 Y_{LM}(\theta, \phi) e^{-i\omega t}. \quad (23)$$

with $L = 0$ (monopole excitations) and $L = 2$ (quadrupole excitations). The corresponding strength function $S_L(\omega)$, which gives the excitation spectrum, is defined by

$$S_L(\omega) = \int_0^\infty dr r^4 \int_0^\infty dr' r'^4 \sum_{\sigma\sigma'} S_L(\omega, r, r'). \quad (24)$$

Another interesting quantity is the transition density $\delta\rho = \rho - \rho_0$, where ρ_0 denotes the density in equilibrium and ρ is the density of the excited system. In the case of zero temperature, where the stationary system is in the ground state $|0\rangle$, the transition density for $\omega = E_j - E_0$ is proportional to

$$\delta\rho(\omega = E_j - E_0, \mathbf{r}) \propto \sum_\sigma \langle j | \hat{\rho}_\sigma(\mathbf{r}) | 0 \rangle. \quad (25)$$

In this case, the sum over i in Eq. (22) reduces to one term ($i = 0$), and therefore the transition density can be obtained from

$$[\delta\rho(\omega = E_j - E_0, \mathbf{r})]^2 \propto \int_{\omega-\delta}^{\omega+\delta} d\omega' S(\omega', \mathbf{r}, \mathbf{r}), \quad (26)$$

where δ is supposed to be sufficiently small to avoid that other states than the selected one ($|j\rangle$) contribute.

B. Superfluid hydrodynamics

At zero temperature, superfluid hydrodynamics provides the equations of motion for the density (per spin state) $\rho(t, \mathbf{r})$ and the irrotational collective velocity field $\mathbf{v}(t, \mathbf{r})$ of the superfluid current (continuity and Euler equations) [17]:

$$\dot{\rho} + \nabla \cdot (\rho \mathbf{v}) = 0, \quad (27)$$

$$\dot{\mathbf{v}} = -\nabla \left(\frac{\mathbf{v}^2}{2} + \frac{V_{ext}}{m} + \frac{\mu_{loc}}{m} \right). \quad (28)$$

These equations can equally be used for fermionic and bosonic systems, only the equation of state, relating the local chemical potential μ_{loc} to the density ρ , must be adapted correspondingly. In the case of weakly interacting fermions, where the density can be regarded as independent of the pairing gap, this equation of state is given by the Thomas-Fermi relation

$$\mu_{loc}(\rho) = \frac{p_F^2}{2m} + g\rho = \frac{\hbar^2 (6\pi^2 \rho)^{2/3}}{2m} + g\rho. \quad (29)$$

In the static (equilibrium) case, Eq. (28) together with this equation of state gives immediately the usual Thomas-Fermi equation for the density profile $\rho_0(\mathbf{r})$,

$$\mu_{loc}[\rho_0(\mathbf{r})] + V_0(\mathbf{r}) = \mu, \quad (30)$$

which is valid in both the normal and the superfluid phase. While the TFA in the normal phase is valid if μ_{loc} is much larger than the discrete level spacing of the trapped system ($\hbar\Omega$ in our case), superfluid hydrodynamics requires in addition that also the pairing gap Δ is large compared with the level spacing, which is much more difficult to satisfy.

Since the superfluid velocity field \mathbf{v} is irrotational, it can be written as a gradient. In order to establish a connection with microscopic quantities, we write it in the form

$$\mathbf{v}(\mathbf{r}) = \frac{\hbar}{m} \nabla \varphi(\mathbf{r}). \quad (31)$$

where φ is related to the phase of the pairing field by $\Delta(\mathbf{r}) = |\Delta(\mathbf{r})| \exp[2i\varphi(\mathbf{r})]$.

In this article we are interested in small-amplitude motion. We therefore split the density and the external potential into their equilibrium values and small deviations, $\rho = \rho_0 + \delta\rho$ and $V_{ext} = V_0 + V_1$, and expand Eqs. (27) and (28) up to linear order in the deviations. In addition, as we did in the preceding subsection, we will specialize to the case of a spherically symmetric harmonic trap and use the corresponding HO units ($\hbar = m = \Omega = 1$), i.e., $V_0 = r^2/2$. We know that for an excitation of the type (23) the solution must be of the form

$$\varphi(t, \mathbf{r}) = \varphi(r) Y_{LM}(\theta, \phi) \exp(-i\omega t) \quad (32)$$

and analogous for $\delta\rho$. Furthermore, we are interested in the eigenmodes of the system, which persist even if

$V_1 = 0$. Then Eqs. (27) and (28) can be transformed into an eigenvalue equation for the eigenfrequencies ω and the corresponding eigenfunctions $\varphi(r)$,

$$\left. \frac{d\mu_{loc}}{d\rho} \right|_{\rho_0} \left(\frac{1}{r^2} (r^2 \rho_0 \varphi')' - L(L+1)\varphi \right) = -\omega^2 \varphi, \quad (33)$$

where f' means df/dr , and an equation for the transition density,

$$\delta\rho = -i\omega \left(\frac{d\mu_{loc}}{d\rho} \right|_{\rho_0} \right)^{-1} \varphi = \frac{-i\omega}{r} \rho_0' \varphi. \quad (34)$$

The numerical solution of Eq. (33) is not difficult. However, in the present article we are only interested in the lowest monopole ($L = 0$) and quadrupole ($L = 2$) modes. For these two modes, the velocity field \mathbf{v} is practically linear in \mathbf{r} , and we can thus obtain a very accurate analytic approximation to the numerical solution. Let us start with the quadrupole mode ($L = 2$). We insert the ansatz $\varphi \approx ar^2$ into Eq. (33), multiply the equation by $\rho_0(r)$ and integrate over d^3r . By this integration the small deviations of the quadratic ansatz from the exact solution of Eq. (33) are averaged out and one thus obtains a very precise prediction for the frequency. After a lengthy calculation we reproduce the well-known result

$$\omega_{L=2} = \sqrt{2}, \quad (35)$$

which is independent of the interaction.

In a similar way we can find an approximation for the eigenfrequency of the lowest monopole mode ($L = 0$). In this case the function φ has the form $\varphi(r) \approx a - br^2$. Inserting this ansatz into Eq. (33), taking the derivative with respect to r in order to get rid of the constant a , multiplying by r and proceeding in the same way as in the case of the quadrupole mode, we finally obtain

$$\omega_{L=0} = 2\sqrt{1 + \frac{3E_{int}}{8E_{pot}}}, \quad (36)$$

where E_{int} and E_{pot} are the interaction and potential energies,

$$E_{int} = \int d^3r g \rho_0^2(\mathbf{r}), \quad E_{pot} = \int d^3r r^2 \rho_0(\mathbf{r}). \quad (37)$$

Contrary to the quadrupole frequency, the monopole frequency depends on the interaction. Since E_{int} is negative, the frequency $\omega_{L=0}$ is slightly lower than twice the trap frequency, 2Ω . Finally, the ratio of the constants a and b , which is needed in order to compute the transition density $\delta\rho$, can be determined from the condition that the integral over $\delta\rho$ must vanish, since the total number of particles stays constant.

C. Vlasov description

Let us now consider a normal Fermi gas just above T_c . In the weakly interacting limit, T_c is very small as compared with the Fermi energy, i.e., except for the fact that

the system is not superfluid, we can neglect temperature effects. We will also assume that the effect of collisions can be neglected. Under this condition the system cannot come to local equilibrium during the collective motion. In order to describe this effect, we will use the Wigner function $f(t, \mathbf{r}, \mathbf{p})$. In equilibrium and within the TFA, this function simply describes a Fermi sphere:

$$f_0(\mathbf{r}, \mathbf{p}) = \Theta(p_F(\mathbf{r}) - p). \quad (38)$$

Out of equilibrium, if the particles do not undergo enough collisions to restore the isotropic momentum distribution, the local Fermi surface will assume a more complicated shape. The equation of motion for the Wigner function is the Vlasov equation

$$\dot{f} = (\nabla V) \cdot (\nabla_p f) - \frac{\mathbf{p}}{m} \cdot (\nabla_r f), \quad (39)$$

where $V(t, \mathbf{r}) = V_{ext}(t, \mathbf{r}) + g\rho(t, \mathbf{r})$ is the total (external+mean-field) potential and ∇_r and ∇_p are acting in coordinate and momentum space, respectively.

Contrary to the hydrodynamic equations in the superfluid phase, it is very difficult to solve the Vlasov equation directly. We are therefore again looking for approximate solutions for the special case of small-amplitude monopole and quadrupole oscillations in a spherical harmonic trap. We will employ the “generalized scaling ansatz” [18], which has been used with great success to describe giant resonances in atomic nuclei and which has also been applied to trapped atomic Fermi gases [6]. In this approach, the possible deformations of the local Fermi surface are restricted to quadrupolar shape. Introducing a small displacement field $\boldsymbol{\xi}(t, \mathbf{r})$, one can write

$$f(t, \mathbf{r}, \mathbf{p}) = f_0(\mathbf{r}', \mathbf{p}'), \quad (40)$$

with

$$\mathbf{r}' = \mathbf{r} - \boldsymbol{\xi}(t, \mathbf{r}), \quad (41)$$

$$\mathbf{p}' = \mathbf{p} - m\dot{\boldsymbol{\xi}}(t, \mathbf{r}) + \nabla_r[\mathbf{p} \cdot \boldsymbol{\xi}(t, \mathbf{r})]. \quad (42)$$

The velocity field is then simply given by $\mathbf{v} = \dot{\boldsymbol{\xi}}$, and the last term in Eq. (42) describes the deformation of the Fermi sphere. For the form of the velocity field we make the same ansatz as before, i.e.,

$$\boldsymbol{\xi}(t, \mathbf{r}) = a \nabla r^2 Y_{LM}(\theta, \phi) e^{-i\omega t}, \quad (43)$$

with $L = 0$ (monopole mode) or $L = 2$ (quadrupole mode). In analogy to the procedure in the preceding subsection, we linearize the Vlasov equation (39) with respect to $\boldsymbol{\xi}$, multiply by $\mathbf{p} \cdot \boldsymbol{\xi}^*$ and integrate over d^3p and d^3r . Using Eqs. (30) we reproduce after a tedious calculation the results originally derived in Ref. [6],

$$\omega_{L=0} = 2\Omega \sqrt{1 + \frac{3E_{kin}}{8E_{pot}}}, \quad \omega_{L=2} = 2\Omega \sqrt{1 - \frac{3E_{kin}}{4E_{pot}}}. \quad (44)$$

Note that the monopole mode has the same frequency in the normal phase as in the superfluid phase. This can be understood as follows. If the displacement field is purely radial ($\xi \propto \mathbf{r}$), as it is the case for the monopole mode, one can see from Eq. (40) that the Fermi surface stays spherical. Therefore hydrodynamics gives the same frequency as the Vlasov equation. The frequency of the quadrupole mode in the normal phase, however, is higher than in the superfluid phase by a factor of approximately $\sqrt{2}$. From Eq. (40) one can see that in this case the Fermi surface gets a quadrupole deformation perpendicular to the deformation of the density profile in coordinate space. This deformation costs energy and therefore increases the frequency of the mode as compared to hydrodynamics.

III. RESULTS

In this section we will compare QRPA and semiclassical results for monopole and quadrupole oscillations in a spherical trap. We are mainly interested in the limits of validity of superfluid hydrodynamics, since this theory is widely used in order to analyze experimental results. For instance, recent experiments showed that the axial breathing mode in a cigar-shaped trap follows the hydrodynamic behavior throughout the BCS-BEC crossover, while the radial breathing mode deviates considerably from the hydrodynamic predictions [19], especially on the BCS side of the crossover region. In this experiment the system was still very strongly interacting even on the BCS side of the crossover (the strongest deviations happened when $k_F|a|$ was of the order of 2), such that our weak-coupling theory (valid for $k_F|a| \ll 1$) cannot directly be compared to that experiment. Nevertheless, it is clear that the limits of validity of hydrodynamics should be clarified. It is known that hydrodynamics works at zero temperature and if the level spacing $\hbar\Omega$ is much smaller than the gap Δ , but both conditions are generally not fulfilled in the experiments. Since experiments cannot be done at zero temperature, it is interesting to see what kind of temperature effects can arise below the critical temperature T_c . The second condition is also very strong, especially if the trap is strongly deformed and the transverse trap frequency is large, and it is therefore important to know up to which ratio $\hbar\Omega/\Delta$ hydrodynamics can be trusted.

A. Temperature dependence

In this subsection we will study how the properties of collective modes change in the small temperature range from zero to the critical temperature T_c . For this investigation we are using the parameter set $\mu = 32 \hbar\Omega$ and $g = -0.965$ (in HO units). With these parameters, the number of particles is approximately 17000 and the gap in the center of the trap at zero temperature is approximately $6 \hbar\Omega$; one can therefore expect that at least at

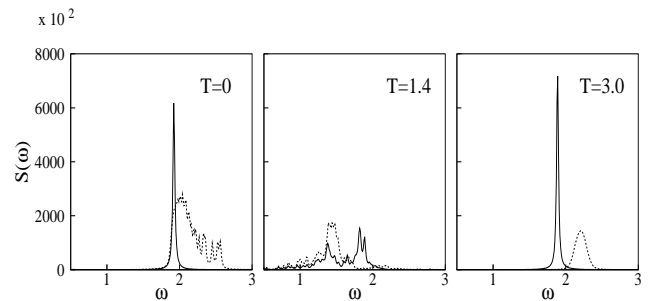


FIG. 1: Free quasiparticle response (dashed line) and QRPA response (solid line) of the monopole excitation as a function of the frequency ω (in units of the trap frequency Ω), for three different temperatures: $k_B T = 0, 1.4 \hbar\Omega$, and $3 \hbar\Omega$ (from left to right).

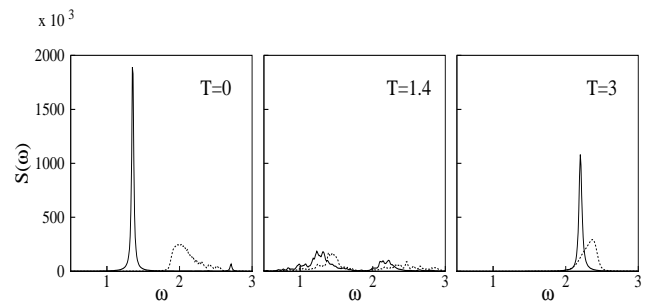


FIG. 2: Free quasiparticle response (dashed line) and QRPA response (solid line) of the quadrupole excitation as a function of the frequency ω (in units of the trap frequency Ω) for three different temperatures: $k_B T = 0, 1.4 \hbar\Omega$, and $3 \hbar\Omega$ (from left to right).

zero temperature hydrodynamics should work very well.

In Figs. 1 and 2 we show the monopole and quadrupole response functions, respectively, for three different values of the temperature. The figures on the left show the response at zero temperature. The solid lines correspond to the QRPA results while the dashed lines represent the free quasiparticle response. In principle, the response function consists of a very large number of discrete levels. For the purpose of graphical presentation, these delta functions must be smeared out, and we therefore intro-

	$T = 0$		$T > T_c$	
	QRPA	hydro.	(Q)RPA	Vlasov
$L = 0$	1.9	1.88	1.9	1.88
$L = 2$	1.4	$\sqrt{2}$	2.2	2.22

TABLE I: Frequencies (in units of the trap frequency Ω) of monopole ($L = 0$) and quadrupole ($L = 2$) modes for $\mu = 32 \hbar\Omega$ and $g = -0.965$ (in HO units) at zero temperature and above T_c . The QRPA results for $T > T_c$ were obtained with $T = 3 \hbar\Omega/k_B$.

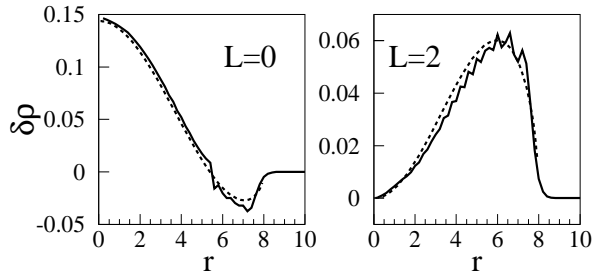


FIG. 3: Transition densities for the collective monopole (left panel) and quadrupole (right panel) modes as a function of r (in units of the oscillator length l_{HO}), at $T = 0$. Solid and dashed lines represent the QRPA and the semiclassical results, respectively.

duce a small imaginary part of $\epsilon = 0.015\Omega$ in the denominators of the correlation functions [see Eq. (22)]. For $T=0$, the QRPA quadrupole response shows one single collective peak whose frequency is very close to that predicted by hydrodynamics (see Table I). The QRPA response is completely different from the free quasiparticle response, which has a broad and almost continuous distribution of strength between $\sim 1.8\Omega$ and $\sim 2.7\Omega$. As has been realized before [11, 13], the threshold of the two-quasiparticle strength is related to the energy of the lowest-lying quasiparticles which are located near the surface of the atomic cloud.

In the case of the monopole mode the good agreement between QRPA and hydrodynamics (Table I) is even more surprising than in the case of the quadrupole mode, since the frequency of the monopole mode is so high that it lies in the two-quasiparticle continuum (see dashed line in Fig. 1) and one would therefore expect a certain amount of Landau damping.

Apart from the study of the frequencies of the collective modes, the comparison between hydrodynamics and QRPA can be extended also to the analysis of the character of such modes. We display in Fig. 3 the transition densities of the two collective modes, which, since the density profile is known, can be related to the velocity field [see Eq. (34)]. The normalization of the QRPA transition density is obtained from the integral of the corresponding peak in the strength function, while that of the semiclassical transition density has been adjusted to the QRPA one. We see that the simple formulas from Sect. II B are in good agreement with the QRPA transition densities. However, the QRPA transition densities exhibit small Friedel-like oscillations, especially near the surface where the gap is small and the local Fermi surface is therefore relatively sharp.

Let us now consider an intermediate temperature between 0 and T_c . For the present set of parameters the critical temperature is $T_c \approx 2.8\hbar\Omega/k_B$; we therefore choose $T = 1.4\hbar\Omega/k_B \approx T_c/2$. As can be seen

in the middle of Figs. 1 and 2, due to the presence of thermally excited quasiparticles the free quasiparticle response starts now already at $\omega = 0$. As a consequence, both the collective monopole and quadrupole modes become strongly fragmented and damped. Qualitatively, this strong Landau damping at temperatures between zero and T_c could be related to the damping mechanism which is responsible for the experimentally observed damping of breathing modes on the BCS side of the BEC-BCS crossover [19]. Interesting is also the double-peak structure which can be seen in the quadrupole response, as if there were two damped modes, one corresponding to the hydrodynamic mode and another one corresponding to the quadrupole mode in the collisionless normal phase (see below). This can be interpreted in the sense of the two-fluid model [20], which states that between $T = 0$ and $T = T_c$ the system effectively behaves as if it consisted of a mixture of normal and superfluid components.

Now we increase the temperature further to $T = 3\hbar\Omega/k_B$, which lies slightly above T_c , i.e., the system reaches the normal phase, but still the temperature is very low compared with the Fermi energy. In the normal phase, the BdG equations become identical to the usual Hartree-Fock equations, and the QRPA becomes equal to the usual RPA. In the case of the monopole mode (right panel of Fig. 1), the QRPA response is almost identical to that at zero temperature (left panel of Fig. 1), although the free quasiparticle response is quite different. Again there is one collective mode having the same frequency as at $T = 0$. This is not very surprising. As mentioned in the preceding section, the Vlasov equation predicts the same frequency as superfluid hydrodynamics, since in the case of the monopole mode there is no deformation of the local Fermi surface. This is different in the case of the quadrupole mode (right panel of Fig. 2). Also here a collective mode reappears, but it is situated at a different frequency than at zero temperature. The higher frequency in the normal phase compared with the superfluid phase is due to the Fermi surface deformation and is well described by the Vlasov equation (cf. Table I).

B. Dependence on the size of the system

Let us now investigate the importance of the discrete level spacing at zero temperature. In the case without superfluidity, the semiclassical $\hbar \rightarrow 0$ limit (TFA in equilibrium and the Vlasov equation in the dynamical case) is known to work very well if the number of particles is sufficiently large. The reason is very simple: The only dimensionless parameter on which corrections can depend is $\hbar\Omega/\mu$, which becomes very small for large numbers of particles. In the current experiments involving $\sim 10^5 - 10^6$ atoms this type of corrections is completely negligible. For our study we choose, as in the preceding subsection, a chemical potential of $\mu = 32\hbar\Omega$. This is large enough to make these corrections small, and the numerical calculations are still tractable. The corresponding numbers

g	N	$\Delta(0)$
-0.965	16500	6.0
-0.8	15000	2.9
-0.7	14300	1.4
-0.636	13900	0.7

TABLE II: Chosen values of the coupling constant g (first column; in HO units) and corresponding results for the number of particles, N (second column), and for the gap at the center of the trap, $\Delta(0)$ (third column; in units of $\hbar\Omega$). The remaining parameters were fixed to $\mu = 32 \hbar\Omega$ and $T = 0$.

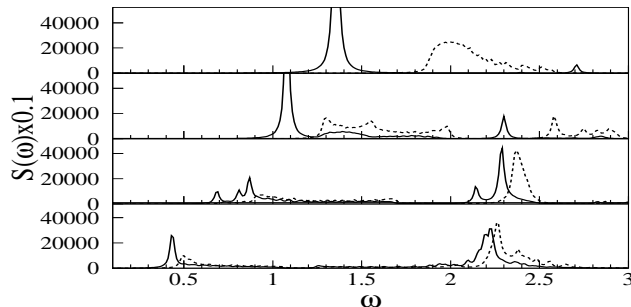


FIG. 4: Unperturbed response (dashed line) and QRPA response (solid line) of the quadrupole excitation as a function of the frequency ω (in units of the trap frequency Ω) for $T = 0$ and $\mu = 32 \hbar\Omega$ and four different values of the coupling constant: $g = -0.965$, $g = -0.8$, $g = -0.7$, and $g = -0.636$ (in HO units; from top to bottom).

of atoms lie between ~ 14000 and ~ 17000 depending on the chosen values of the coupling constant g due to the Hartree field (see Table II).

In the case of superfluidity, however, another dimensionless parameter becomes important, which is $\hbar\Omega/\Delta$. Since in the BCS phase $\Delta \ll \mu$, this parameter is not necessarily small even if the number of particles is very large. In order to study the validity of hydrodynamics as a function of $\hbar\Omega/\Delta$, we change Δ by varying the coupling constant g between -0.636 and -0.965 (in HO units). As a measure for Δ we take its value at the center of the trap, $\Delta(0)$. The values of $\Delta(0)$ corresponding to the different coupling constants are listed in Table II.

We are now going to analyze the finite-size effects on the quadrupole response function by using the different values of the coupling constant listed in Table II. Note that, since we are using HO units, changing the coupling constant $g \propto a/l_{HO}$ is equivalent to changing the oscillator length l_{HO} and thus the radius of the cloud $R = \sqrt{2\mu/\hbar\Omega} l_{HO}$. Anyway, as argued above, the important parameter for finite-size effects is the ratio $\hbar\Omega/\Delta(0)$ and not the cloud size itself.

For the strongest coupling, $g = -0.965$ (in HO units), the central value of the gap, $\Delta(0)$, is large compared with $\hbar\Omega$, and hydrodynamics works almost perfectly at zero temperature, as we have already seen in the preceding

subsection. Fig. 4 shows, from top to bottom, the evolution of the quadrupole response at $T = 0$ for decreasing coupling constant g , i.e., for increasing importance of the discrete level spacing. Besides the QRPA response (solid lines), we also show the free quasiparticle response (dashed lines). For $g = -0.8$ (in HO units), the gap at the center is still larger than $\hbar\Omega$ by a factor of three, but now we find considerable deviations of the QRPA response from the hydrodynamic result. Since the free quasiparticle response is now shifted to lower frequencies, the hydrodynamic mode becomes fragmented, which experimentally would show up as damping effect, and its frequency ($\omega \approx 1.1 \Omega$) lies below the hydrodynamic prediction ($\sqrt{2}\Omega$). For $g = -0.7$ and $g = -0.636$ (in HO units), the central value of the gap is comparable to $\hbar\Omega$ and it is clear that hydrodynamics must fail. Indeed, the QRPA response becomes more and more similar to the free quasiparticle response which in the case of weak pairing looks very different from the strong-pairing case. The double-peak structure is a consequence of the two types of transitions which are allowed by the selection rules of the harmonic oscillator, i.e., transitions inside an oscillator shell ($\delta N = 0$, where N denotes the number of oscillator quanta) and transitions with $\delta N = 2$. As the interaction decreases, the strength of the $\delta N = 0$ transitions becomes less important while the $\delta N = 2$ transitions become stronger. This can be understood from the fact that in the limit of a noninteracting harmonic oscillator without pairing ($g \rightarrow 0$) the $\delta N = 0$ transitions are forbidden by Pauli principle and only the $\delta N = 2$ transitions survive. In this limit the response has a single peak at $\omega = 2\Omega$, in exact agreement with the prediction from the Vlasov equation [23]. In the semiclassical language, one can say that in this case the pairing is too weak to restore the spherical shape of the Fermi sphere during the oscillation, and therefore one finds the normal collisionless frequency instead of the hydrodynamical one.

IV. SUMMARY AND CONCLUSIONS

In this article we have studied the properties of collective monopole and quadrupole modes in superfluid Fermi gases in the BCS phase ($k_F|a| \ll 1$, $a < 0$) in a spherical harmonic trap. Having briefly recalled the quantum mechanical and semiclassical formalisms (QRPA, hydrodynamics, Vlasov equation), we presented numerical results and compared the different formalisms. Our main interest was focused on two types of effects: temperature and finite-size effects. Both cannot be treated within the semiclassical approaches available in the present literature, and they can therefore only be studied in the framework of the fully microscopic QRPA formalism.

In the case of a sufficiently large system (large meaning $\Delta \gg \hbar\Omega$), superfluid hydrodynamics can be used to describe the properties of collective modes at zero temperature. Our results confirm earlier findings [11] which show that already for parameters which lead to $\Delta(0) = 6\hbar\Omega$

the extremely simple theory of superfluid hydrodynamics is in almost perfect agreement with the numerically heavy QRPA method. This is not only true for the frequencies, but also for the transition densities, i.e., the velocity fields associated with the collective modes. However, experiments can never be done at zero temperature. The critical temperature T_c being extremely low, it is clear that already at very low temperatures between 0 and T_c the properties of the collective modes must undergo dramatic changes. This is evident if the hydrodynamic frequency ($T = 0$) is different from that in the collisionless normal phase ($T = T_c$), like in the case of the quadrupole mode. In the case of the monopole mode we also find a strong temperature dependence, although its frequency at $T = 0$ is the same as at $T = T_c$. In the intermediate temperature range between 0 and T_c the collective modes exhibit strong Landau damping. When the critical temperature is reached, the damping disappears and the collective modes can be very well described by the semiclassical Vlasov equation within the generalized scaling approximation.

It is interesting to compare these temperature effects with those found previously in the case of the twist mode [21], which is an excitation where the upper hemisphere rotates against the lower one. Near T_c , the behavior is rather similar: At $T = T_c$ the twist mode is a collective mode which can be described by the generalized scaling approximation to the Vlasov equation and whose frequency is slightly higher than the trap frequency. If the temperature is lowered, the twist mode becomes strongly damped, like the quadrupole and monopole modes. However, an important qualitative difference appears near zero temperature. Since the velocity field of the twist mode cannot be written as a gradient, the twist mode

disappears completely at zero temperature, whereas the quadrupole and monopole modes have an irrotational velocity field and they reappear at zero temperature as hydrodynamic modes. In the case of the twist mode, the disappearance of the $1/\omega$ weighted integrated strength could be well described within a rather simple two-fluid model [21, 22]. It remains to be studied if a generalization of the two-fluid model to the dynamical case can also explain the damping of the quadrupole and monopole modes and the two-peak structure in the quadrupole response function at temperatures between 0 and T_c .

In addition to temperature effects, we studied how the properties of the quadrupole mode change at zero temperature when the condition for the validity of the hydrodynamic approach, $\Delta \gg \hbar\Omega$, is no longer satisfied. For parameters leading to $\Delta(0) \approx 3\hbar\Omega$ the QRPA already shows considerable deviations from the hydrodynamic theory. In the case of the quadrupole mode, the frequency for these parameters is found to be lower by 20% than the hydrodynamic prediction, and a certain fragmentation of the excitation spectrum (i.e., damping of the collective mode) can be observed. If $\Delta(0) \approx \hbar\Omega$, the hydrodynamic mode has more or less disappeared. At the same time, a fragmented strength appears in the excitation spectrum near the frequency of the collective quadrupole mode in the normal collisionless phase.

These results should be kept in mind when frequencies of collective modes measured in experiments with strongly deformed traps are compared with the hydrodynamic predictions. Due to the strong deformation, the radial trap frequency Ω_r is often much higher than the axial one, Ω_z . Even in the case of strong pairing, the gap might be of the order of, say, $3\hbar\Omega_z$, and considerable deviations from hydrodynamics are possible.

-
- [1] M.H. Anderson, et al., *Science* **269**, 198 (1995); K.B. Davis, et al., *Phys. Rev. Lett.* **75**, 3969 (1995); C.C. Bradley, et al., *Phys. Rev. Lett.* **75**, 1687 (1995).
 - [2] M.W. Zwierlein, et al., *Phys. Rev. Lett.* **91**, 250401 (2003)
 - [3] K.M. O'Hara, et al., *Science* **298**, 2179 (2002).
 - [4] C. Chin, et al., *Science* **305**, 1128 (2004).
 - [5] J. Kinast, et al., *Phys. Rev. Lett.* **92**, 150402 (2004).
 - [6] C. Menotti, P. Pedri, and S. Stringari, *Phys. Rev. Lett.* **89**, 250402 (2002).
 - [7] S. Stringari, *Europhys. Lett.* **65**, 749 (2004).
 - [8] M.A. Baranov and D.S. Petrov, *Phys. Rev. A* **62**, 041601 (2000).
 - [9] P.-G. de Gennes, *Superconductivity of Metals and Alloys* (Benjamin, New York, 1966).
 - [10] P.W. Anderson, *Phys. Rev.* **112**, 1900 (1958).
 - [11] G.M. Bruun and B.R. Mottelson, *Phys. Rev. Lett.* **87**, 270403 (2001).
 - [12] G.M. Bruun, *Phys. Rev. Lett.* **89**, 263002 (2002).
 - [13] Y. Ohashi and A. Griffin, preprint cond-mat/0503641 (2005).
 - [14] G. Bruun, Y. Castin, R. Dum, and K. Burnett, *Eur. Phys. J. D* **7**, 433 (1999).
 - [15] A. Bulgac and Y. Yu, *Phys. Rev. Lett.* **88**, 042504 (2002).
 - [16] M. Grasso and M. Urban, *Phys. Rev. A* **68**, 033610 (2003).
 - [17] M. Cozzini and S. Stringari, *Phys. Rev. Lett.* **91**, 070401 (2003).
 - [18] P. Ring and P. Schuck, *The Nuclear Many-Body Problem* (Springer-Verlag, Berlin, 1980).
 - [19] M. Bartenstein, et al., *Phys. Rev. Lett.* **92**, 203201 (2004).
 - [20] A.J. Leggett, *Phys. Rev.* **140**, A 1869 (1965); *Phys. Rev.* **147**, 119 (1966).
 - [21] M. Grasso, M. Urban, and X. Viñas, *Phys. Rev. A* **71**, 013603 (2005).
 - [22] M. Urban, *Phys. Rev. A* **71**, 033611 (2005).
 - [23] In the case of a non-interacting harmonic oscillator, as well as in the case of a harmonic oscillator with separable quadrupole-quadrupole interaction, the Vlasov equation is known to reproduce exactly the quantum mechanical solution.